Total component transformation of corn stalk to ethyl levulinate assisted by ionic liquid pretreatment

Yixiang Wang
Qingdao University of Science and Technology
Xiao Zheng
Qingdao University of Science and Technology
Xiaoqi Lin
Qingdao University of Science and Technology
Xuebin Liu
Qingdao University of Science and Technology
Dezhi Han
Qingdao University of Science and Technology
Qinqin Zhang
qqzhang@qust.edu.cn

Qingdao University of Science and Technology

Research Article

Keywords: Biomass, Corn stalk, Liquefaction, Ionic liquid, Ethyl levulinate

Posted Date: September 2nd, 2023

DOI: https://doi.org/10.21203/rs.3.rs-3301698/v1

Additional Declarations: No competing interests reported.

Version of Record: A version of this preprint was published at Cellulose on March 28th, 2024. See the published version at https://doi.org/10.1007/s10570-024-05818-8.

Abstract

The conversion from widely available and inexpensive crop stalk to high-value platform chemicals through highly selective catalytic liquefaction under mild conditions is one of the effective ways for biomass utilization. In this work, a two-step "lignin-first" process was used to remove lignin from corn stalk (CS) with protonic ionic liquid [B2-HEA][OAc] as the pretreatment agent, followed by targeted conversion of lignocellulosic biomass to ethyl levulinate (EL) using alcoholic liquefaction technology. The optimal pretreatment conditions of CS and liquefaction conditions for the conversion of pretreated CS to EL were investigated. The highest recoveries of cellulose and hemicellulose were 83.78% and 67.20% as well the delignification rate of lignin was 70%, respectively, at the maximum biomass loading (liquid-solid ratio of 10:1), pretreatment temperature of 130°C and pretreatment time of 5 h. And the maximum EL yield of was up to 39.93% at the liquefaction temperature of 190°C with the liquefaction time of 90 mins. Meanwhile, the crystallinity, thermal stability, functional group and morphology of CS, pretreated CS and liquefied residue were carried out using x-ray diffractometer, thermal gravimetric analyzer, fourier transform infrared spectrometer and scanning electron microscope. It was suggested the lignin was effectively removed from corn stalk by ionic liquid pretreatment. Compared to original CS, the cellulose crystallinity index (CrI) of pretreated CS was reduced from 37.17–35.39%, and the surface of the pretreated CS became rough because of regular structure in cellulose broken by the ionic liquid.

1 Introduction

The development of the global economy faces mounting challenges in sectors like energy, food and agriculture as it seeks to combat global warming and reduce fossil fuel dependence. The COVID-19 pandemic from late 2019 has exacerbated these challenges. Rising fuel costs and heightened concerns over fossil fuel environmental impacts have compelled researchers to explore renewable biofuels production from lignocellulosic biomass more urgently (Islam et al., 2020). Bio-refining of lignocellulosic biomass shows immense potential for converting plant-based wastes into industrial products and renewables (Abraham et al., 2020). Main sources are forestry and agricultural residues, dedicated energy crops, organic municipal wastes, and industrial waste streams (wood, paper, pulp) (Roy et al., 2021).

According to surveys, around 81.5 billion tons of lignocellulosic biomass is produced globally each year, but only 4.5% is effectively utilized. Of this, 3.8% comes from forests, farms and grasslands, while the remaining 0.7% are agricultural crop residues (Dahmen et al., 2019). Traditionally, lignocellulosic biomass has been used for cooking, heating, construction and paper industries. For environmental sustainability, current research aims to produce biofuels, biochemicals and other industrial products from lignocellulosic biomass, reducing dependence on fossil fuels (Biddy et al., 2016; Patel et al., 2019; Usmani et al., 2020). As the most abundant renewable feedstock, lignocellulosic biomass can potentially meet sustainable chemical and energy needs, lowering the high reliance on fossil fuels. Therefore, efficient conversion processes need to be developed to tap into this vast unused resource. With emerging bio-refining technologies, lignocellulosic biomass promises to enable a transition from fossil fuels to sustainable bio-based fuels, chemicals and materials.

Lignocellulosic biomass has a complex three-dimensional structure, with the cellulose skeleton intricately wrapped by hemicellulose and stress-resistant lignin bound by hydrogen and covalent bonds (Zhao et al., 2012). This rigid structure makes lignocellulose highly resistant to degradation, requiring targeted pretreatments to unlock biomass conversion. Currently, various pretreatment methods have been developed to overcome lignocellulose's structural inflexibility and improve carbohydrate accessibility. These include acid (Jędrzejczyk et al., 2019), alkaline (Keshav et al., 2016), organic solvent(Capolupo and Faraco, 2016) and ammonia fiber explosion pretreatments (Baral and Shah, 2017). Physical disruption via milling or extrusion is often incorporated as the first step before chemical pretreatments to aid in biofuel conversion (Hendriks and Zeeman, 2009). Although traditional pretreatment techniques effectively decompose lignocellulosic structure, they often cause environmental pollution and carbohydrate loss (Balan, 2014). Ionic liquids have emerged as a green solvent alternative, composed of large organic cations and small anions that can selectively dissolve lignocellulose by tuning their structure. As they exist as liquids at room temperature with negligible vapor pressure and 99% recovery, ionic liquids can disrupt the intermolecular hydrogen bonds in polysaccharides and lignin (Samayam and Schall, 2010). In a typical process, biomass is pretreated with ionic liquids at 90–130°C and ambient pressure for 1–24 hours, followed by thorough washing before enzymatic hydrolysis (Brodeur et al., 2011). The anion interacts with cellulose hydrogen bonds, disrupting its crystalline structure to yield amorphous cellulose that is more readily enzymatically hydrolyzed. However, ionic liquids can cause irreversible enzyme inactivation over time, necessitating careful recycling and recovery (Turner et al., 2003).

Ionic liquids have a high capacity to dissolve and decrystallize cellulose, overcoming the recalcitrance of lignocellulosic biomass and enhancing enzymatic hydrolysis (Brandt et al., 2013). They exhibit high thermal stability unlike traditional toxic organic solvents with low cellulose solubility. Most ionic liquids also have negligible vapor pressure, making handling and recovery easier during pretreatment. Moreover, their tunable cation and anion structures allow specific designs for targeting biomass components (Olivier-Bourbigou et al., 2010). However, high costs currently limit viability. Protic ionic liquids, generated by one-step proton transfer between Brønsted acids and bases, have simpler synthesis, lower costs and faster production than aprotic types (Chen et al., 2014). This enables selective lignin extraction for value-added products (Rocha et al., 2017).

In this work, a low-cost protic ionic liquid was synthesized as a pretreatment solvent. Corn stalks (CS) were used as the raw material for pretreatment to separate lignin and obtain polysaccharide-rich pretreated CS. Optimal pretreatment conditions were determined by investigating temperature and time effects. Ethyl levulinate (EL) was then prepared by catalytically transforming the pretreated CS using a self-made ionic liquid as of $[C_3H_6SO_3Hmim]HSO_4$ the catalyst. Optimal reaction conditions for EL production were found by evaluating temperature, time and catalyst loading.

2 Experimental

2.1 Materials

CS were collected from Rizhao, Shandong province, China. ethanol was purchased from Sinopharm Chemical ReagentCo., Ltd. Diethanolamine (98 wt%) was purchased from Yantai Yuandong Fine Chemicals Co., Ltd. Acetic Acid was purchased from Tianjin Aopusheng Chemical Sales Co., Ltd. Concentrated sulfuric acid (98 wt%) was purchased from Yantai Yuandong Fine Chemicals Co., Ltd. Trichloromethane was purchased from Tianjin Beilian Fine Chemicals Development Co., Ltd. The protic ionic liquid $[C_3H_6SO_3Hmim]HSO_4$ was synthesized in the laboratory.

2.2 Synthesis of ionic liquid [B2-HEA][OAc]

Double (2-hydroxyethyl) ammonium acetate ionic liquid [B2-HEA][OAc] was synthesized via an acid-base reaction between the Brønsted acid glacial acetic acid and the Brønsted base diethanolamine. Equimolar ratios (1:1) of the reagents were used, with 2.5 mol of each. The diethanolamine was first placed in a 1 L round-bottom flask immersed in an ice bath at 0–5°C under atmospheric pressure. Glacial acetic acid was then added dropwise with constant stirring over 30 mins. After 2–4 h, pure ethanol of 120 mL was added to the funnel to rinse acetic acid l. The mixture was continuously stirred for 6 hours to allow sufficient proton exchange. The resulting ionic liquid was stored at room temperature until further use.

2.3 Pretreatment of CS by [B2-HEA][OAc]

For pretreatment, 1 g of CS and 10 g of [B2-HEA][OAc] were added to a 100 ml round-bottomed flask. After thorough mixing, the flask was immersed in an oil bath and preheated to the pretreatment temperature (110–150°C). After the desired reaction time, the flask was cooled in an ice bath. The pretreated samples were washed three times with 25 mL ethanol, filtered under vacuum, and washed again with 30 mL deionized water. The pretreated CS was dried for further catalytic conversion. The liquid fraction was centrifuged at 7500 rpm for 30 mins to precipitate lignin. The lignin was thoroughly washed with deionized water, freeze-dried at -50°C for 24 h, and stored for further analysis.

2.4 Analysis of composition

The chemical composition of untreated and pretreated CS samples was analyzed using a two-step acid hydrolysis process based on the National Renewable Energy Laboratory (NREL) protocol. Acid hydrolysates were generated and the released monosaccharides quantified by high-performance liquid chromatography (HPLC) using an Aminex HPX-87P column (Agilent, Santa Clara, USA). The mobile phase was ultra-pure water with a 0.6 $mL{\cdot}min^{-1}$ flow rate at 85°C. The solid residue from hydrolysis was used to determine acid-soluble and acid-insoluble lignin content. The compositional content was calculated using Eq. (1).

$$\text{Composition content } (\%) = \frac{\mathrm{m}_a}{\mathrm{M_A}} \times 100\% \quad (1)$$

Where, m_a indicates the quality of recovered glucose/xylose/lignin and M_A indicates the quality of glucose/xylose/lignin in the CS, respectively.

2.5 Catalytic conversion of pretreated CS to EL

In this experiment, 4 g of CS, a specified amount of $[C_3H_6SO_3Hmim]HSO_4$, and 100 mL of pure ethanol were added to a 250 mL high-pressure reactor. The reaction system was purged with nitrogen gas to remove air before sealing. The reaction proceeded with continuous stirring at 500 rpm for 90–150 mins at 180–220°C. After the reaction, the reactor was cooled in an ice water bath and quenched for 20 mins. The residual solids (RS) were collected by filtration, thoroughly washed with ethanol, and dried at 105°C for further analysis. The filtrate and washing solution were combined and the ethanol was removed by rotary evaporation. 20 mL of chloroform was added to the concentrate three times and further evaporated to obtain the EL. The RS yield, CS conversion rate, and product yield based on converted CS were calculated using Equations (2), (3), and (4), respectively.

$$\text{RS yield } (\%) = \frac{\mathrm{m_{RS}}}{\mathrm{m_{CS}}} \times 100\%$$

2

$$\text{Conversion rate } (\%) = 1 - \text{RS yield}$$

3

$$\text{EL yield } (\%) = \frac{\mathrm{m_{EL}}}{\mathrm{m_{CS}} \times (\text{Conversion rate})} \times 100\%$$

4

Where, m_{RS}, m_{CS} and m_{EL} are the mass of RS (g), CS (g) and EL (g), respectively.

2.6 Characterization

The crystallinity of the sample was determined by X-ray diffraction (XRD) using a D/max 2500 diffractometer (Rigaku Corporation, Tokyo, Japan) at a tube voltage and current of 40 kV and 20 mA, respectively. The scanning range was 10°-40° with a step size of 2°.

The thermal properties of CS, pretreated CS, and RS were analyzed by thermogravimetric analysis (TGA) using a TGA/DSC 1SF instrument (Mettler Toledo, Zurich, Switzerland). Samples were heated from 30 to 900°C at a rate of 10°C·min^{-1} under a nitrogen gas flow of 60 mL·min^{-1} as both purge and protective gas.

Fourier transform infrared (FTIR) spectra of CS, pretreated CS, and RS were recorded using a Bruker VERTEX 70 FTIR spectrometer (Bruker Optik GmbH, Ettlingen, Germany) equipped with a total reflection (ATR) accessory. The spectra were collected over a wavenumber range of 4000 – 600 cm^{-1} at a resolution of 2 cm^{-1}.

The micromorphology of CS, pretreated CS, and RS was observed using a Hitachi S-4800 scanning electron microscope (SEM) operated at an acceleration voltage of 5.0 kV.

3 Results and discussion

3.1 Effect of pretreatment conditions on composition content of pretreated CS

Insufficient concentration of [B2-HEA][OAc] resulted in incomplete dissolution of lignin, which inhibited the efficiency of subsequent catalytic conversion. However, increasing the ionic liquid concentration also increases costs, so the concentration should be optimized for industrial production. As shown in Fig. 1, the effects of pretreatment temperature and time on the composition content of pretreated CS were investigated under maximum biomass loading, in order to balance reaction efficiency and recovery rate.

Pretreatment temperature and time greatly affect pretreatment efficiency. Lignin, an aromatic polymer, is the main obstacle to lignocellulosic biomass degradation (Rahikainen et al., 2013). Increasing pretreatment time and temperature improves lignin extraction. As seen in Fig. 1, under optimal pretreatment conditions of 5 h at 130°C, high cellulose and hemicellulose yields of 52.22% and 30.18%, respectively, as well as a lignin delignification rate of 85.88% were achieved.

Increasing pretreatment temperature and time led to gradual increases in cellulose and hemicellulose yields, along with improved lignin removal. At a constant temperature of 130°C, recovery rates of glucan and xylan, and lignin removal all increase with reaction times from 1 h to 5 h. This can be attributed to the high solubility of lignin in [B2-HEA][OAc]. Higher temperatures cause faster cellulose expansion as the hydrogen bonds in its three-dimensional structure are broken due to increased kinetic energy (da Costa Lopes et al., 2013). When pretreatment time is 2 h, cellulose yield increases with temperature, rising by ~ 20% as temperature increases from 110°C to 150°C. This indicates selective lignin removal while retaining most glucan and xylan after [B2-HEA][OAc] pretreatment, which is beneficial for improving subsequent EL yield. However, at 150°C, cellulose content decreased with longer treatment times. This partial cellulose hydrolysis is caused by excessive pretreatment time at high temperatures. Temperature also significantly affects hemicellulose content. At 5 h, hemicellulose content at 150°C is only half that at 110°C. This can be attributed to the amorphous structure of hemicellulose. At high temperatures, the alcoholysis degree increases, lowering hemicellulose content with longer pretreatment.

3.2 Research on liquefaction conditions

Based on the investigation of pretreatment conditions, pretreated CS obtained at 130°C for 5 hours was selected as the feedstock for catalytic liquefaction. The influence of catalyst dosage on CS conversion rate and EL yield was investigated as shown in Fig. 2a. With the increase of catalyst dosage, the conversion rate of CS and EL production first increases and then decreases. More catalyst provides more active sites, accelerating CS conversion to EL. However, above 8 mmol catalyst, the higher acid

concentration promotes sugar and derivative condensation into humins (Chen et al., 2020), inhibiting CS-to-EL conversion and decreasing EL yield.

The effects of reaction temperature on CS conversion rate and EL yield were studied, as shown in Fig. 2b. Rising reaction temperature initially increases both CS conversion and EL yield, which peaked at 190°C before slightly decreasing. Above 190°C, intermediate products likely underwent increased condensation or even partial carbonization, decreasing EL yield. This is supported by the decrease in CS conversion rate above 190°C.

The effect of reaction time on CS conversion rate and EL yield is shown in Fig. 2c. The trends for CS conversion and EL yield over time are similar to those for temperature. However, EL yield does not decrease with longer reaction times. Prolonged reaction time likely promotes complete EL formation at 190°C, as the esterification between levulinic acid and ethanol to produce EL is reversible. Longer times ensure full progression of the esterification reaction.

3.3 Crystallinity

Pretreatment removed amorphous hemicellulose, lignin, and some amorphous cellulose, which typically increases substrate crystallinity. However, XRD (Fig. 3) shows the crystallinity index (CrI) of pretreated CS decreases from 37.17–35.39% compared to original CS. This reduction is attributed to the damage of the natural degradation barrier formed by lignin and hemicellulose. Their hydrogen bonding with cellulose becomes weaken, and more free hydroxyl groups are formed (Yang et al., 2019), allowing more cellulose to be exposed and further degraded, leading to a decrease in crystallinity.

3.4 FTIR analysis

Figure 4 shows the FTIR spectra of CS, pretreated CS, and RS. The broad strong absorption peaks at 3600 – 3200 cm^{-1} are attributed to the stretching vibrations of the hydroxyl group. The absorption peak from 1700 cm^{-1} to 1650 cm^{-1} corresponds to the bending vibration of water. The peaks at 2929 cm^{-1} and 2873 cm^{-1} represent the characteristic absorption of $–CH_2$ and $–CH_3$ groups. The presence of an infrared absorption peak at 1645 cm^{-1} indicates the adsorption of tightly bound water in the amorphous region of cellulose. The peaks at 1085 cm^{-1} and 927 cm^{-1} originate from the skeleton vibration of C–O–H bending and cellulose β-1,4-glycosidic linkages, respectively. The peaks at 1235 cm^{-1} and 1737 cm^{-1} correspond to the C–O bond in xylan and the C = O ester bond in the xylan/lignin-carbohydrate complex (LCC) structure. Compared to the raw material, the absorption intensity at these two wavenumbers decreased significantly after [B2-HEA][OAc] treatment due to the removal of hemicellulose from the amorphous region. The absorption peaks at 899 cm^{-1} and 1099 cm^{-1} arise from amorphous cellulose and crystalline cellulose. The similar intensities of these two peaks before and after pretreatment indicate negligible degradation of cellulose during the process. Furthermore, the absence of peaks related to cellulose and hemicellulose in the RS spectrum implies that these components were almost completely degraded during catalytic liquefaction.

3.5 Thermal behavior

Figure 5 shows the TGA curves of CS (a), pretreated CS (b) and RS (c). The thermal decomposition of all samples occurs in three main stages. In stage I, weight loss peaks from room temperature to 150°C are due to evaporation of moisture, adsorbed water molecules, and possibly volatile compounds. The principal pyrolysis temperature range of cellulose and hemicellulose is 200–380°C. The pyrolysis temperature of pretreated CS is approximately 70–80°C higher than that of original CS. Since most hemicellulose is removed after pretreatment while a large amount of crystalline cellulose is retained, the thermal stability of pretreated CS exceeds that of the original CS. The TGA curve of pretreated CS exhibits only one peak (299–303°C) in stage II, indicating degradation of hemicellulose and cellulose during pretreatment. Lignin begins decomposing at 200–400°C, primarily due to cleavage of ether bonds. As the temperature rises above 420°C, the thermal gravimetric rate of the RS is lower, likely because the main volatile compounds released from the branched aromatic structure of lignin are alcohols, uronic acids and phenols.

3.6 Morphology analysis

As shown in Fig. 6, the structural changes of CS, pretreated CS and LR are studied by SEM. The surface morphology of CS is smooth and compact, which restricts the separation and further transformation of components. The surface of the pretreated CS becomes rough, which structural firmness is damaged after ionic liquid pretreatment. The fiber is exposed and short fiber structure is found, indicating that the connection within the CS structure is broken. In addition, a small number of particles (lignin and/or pseudo-lignin) are deposited on the surface of the pretreated CS, indicating that ionic liquid pretreatment can effectively remove lignin.

Figure 6 shows SEM images illustrating the structural changes in CS, pretreated CS and RS. The surface morphology of original CS is smooth and compact, which restricts the separation and further transformation of components. After IL pretreatment, the surface of pretreated CS becomes rough as the structural integrity is disrupted. The exposure of fibers and presence of short fiber structures indicates that connections within the CS structure are broken. Additionally, some particles (lignin and/or pseudo-lignin) are deposited on the surface of pretreated CS, suggesting that the ionic liquid pretreatment can effectively remove lignin. The RS lacks an obvious fiber bundle structure, indicating it consists mostly of undegradable lignin.

4 Conclusion

The ionic liquid [B2-HEA][OAc] was successfully synthesized via an acid-base reaction using equimolar amounts (1:1 molar ratio) of the Brønsted acid glacial acetic acid and the Brønsted base diethanolamine. The optimal solid-liquid ratio of 1:10 was determined by exploring the maximum biomass loading capacity of [B2-HEA][OAc] for CS. CS was pretreated with [B2-HEA][OAc] as the solvent to investigate the relationship between pretreatment conditions and substrate chemical composition. The results showed

high lignin removal rates of 82.96%-90.78% from the substrates, while 83.40%-85.46% of the original cellulose and hemicellulose remained. The optimal pretreatment temperature and time were 130°C and 5 h, respectively.

Furthermore, the pretreated CS was catalyzed using $[C_3H_6SO_3Hmim]HSO_4$ as the catalyst under optimal conditions of 8 mmol catalyst dosage, 190°C reaction temperature, and 90 min reaction time, obtaining a high EL yield of 39.93%. Compared to the original CS, the CrI of the pretreated CS was reduced from 37.17–35.39%, and its thermal stability was improved. Additionally, the structural integrity of the CS was disrupted after [B2-HEA][OAc] pretreatment.

Declarations

Acknowledgment

The authors acknowledge the department of the National Natural Science Foundation of China [No. 51803107] and Natural Science Foundation of Shandong Province [No. ZR2022MB019].

Author contributions

All authors contributed to the study conception and design. Material preparation, data collection and analysis were performed by Xiao Zheng, Xiaoqi Lin, Xuebin Liu, Dezhi Han and Qinqin Zhang. The first draft of the manuscript was written by Yixiang Wang and all authors commented on previous versions of the manuscript. All authors read and approved the final manuscript.

Funding

This work was supported by the National Natural Science Foundation of China [No. 51803107] and Natural Science Foundation of Shandong Province [No. ZR2022MB019].

Data availability

The datasets used and/or analyzed during the current study are available from the corresponding author on reasonable request.

Conflict of interest

The authors have no relevant financial or non-financial interests to disclose.

Ethical approval

We declare that there is no financial or personal relationship between us and other people or organizations that may have an inappropriate impact on this work. Consent has been taken from all the authors for participation in this study.

Consent for publication

Consent has been taken from all the authors for publication of this manuscript.

References

1. Abraham A, Mathew AK, Park H, Choi O, Sindhu R, Parameswaran B, Pandey A, Park JH, Sang BI (2020) Pretreatment strategies for enhanced biogas production from lignocellulosic biomass. Bioresour. Technol. 301: 122725. https://doi.org/10.1016/j.biortech.2019.122725.
2. Balan V (2014) Current challenges in commercially producing biofuels from lignocellulosic biomass. ISRN Biotechnol. 2014: 463074. https://doi.org/10.1155/2014/463074.
3. Baral NR, Shah A (2017) Comparative techno-economic analysis of steam explosion, dilute sulfuric acid, ammonia fiber explosion and biological pretreatments of corn stover. Bioresour. Technol. 232: 331-343. https://doi.org/10.1016/j.biortech.2017.02.068.
4. Biddy MJ, Davis R, Humbird D, Tao L, Dowe N, Guarnieri MT, Linger JG, Karp EM, Salvachúa D, Vardon DR, Beckham GT, (2016) The techno-economic basis for coproduct manufacturing to enable hydrocarbon fuel production from lignocellulosic biomass. ACS Sustain. Chem. Eng. 4: 3196-3211. https://doi.org/10.1021/acssuschemeng.6b00243.
5. Brandt A, Gräsvik J, Hallett JP, Welton T (2013) Deconstruction of lignocellulosic biomass with ionic liquids. Green Chem. 15: 550-583.https://doi.org/10.1039/C2GC36364J
6. Brodeur G, Yau E, Badal K, Collier J, Ramachandran KB, Ramakrishnan S (2011) Chemical and physicochemical pretreatment of lignocellulosic biomass: a review. Enzyme Res. 2011: 787532. https://doi.org/10.4061/2011/787532.
7. Capolupo L, Faraco V (2016) Green methods of lignocellulose pretreatment for biorefinery development. Appl. Microbiol. Biotechnol. 100: 9451-9467. https://doi.org/10.1007/s00253-016-7884-y.
8. Chen L, Sharifzadeh M, Dowell NM, Welton T, Shah N, Hallett JP (2014) Inexpensive ionic liquids: [HSO_4] -based solvent production at bulk scale. Green Chem. 16: 3098-3106. https://doi.org/10.1039/C4GC00016A.
9. Chen W, Zhang Q, Lin X, Jiang K, Han D (2020) The degradation and repolymerization analysis on solvolysis liquefaction of corn stalk. Polymers 12: 2337. https://doi.org/10.3390/polym12102337.
10. da Costa Lopes AM, Joao KG, Rubik DF, Bogel-Lukasik E, Duarte L., Andreaus J, Bogel-Lukasik R (2013) Pre-treatment of lignocellulosic biomass using ionic liquids: wheat straw fractionation. Bioresour. Technol. 142: 198-208. https://doi.org/10.1016/j.biortech.2013.05.032.

11. Dahmen N, Lewandowski I, Zibek S, Weidtmann A (2019) Integrated lignocellulosic value chains in a growing bioeconomy: Status quo and perspectives. GCB Bioenergy 11: 107-117. https://doi.org/10.1111/gcbb.12586.
12. Hendriks AT, Zeeman G (2009) Pretreatments to enhance the digestibility of lignocellulosic biomass. Bioresour. Technol. 100: 10-18. https://doi.org/10.1016/j.biortech.2008.05.027.
13. Islam MK, Wang H, Rehman S, Dong C, Hsu HY, Lin CSK, Leu SY (2020) Sustainability metrics of pretreatment processes in a waste derived lignocellulosic biomass biorefinery. Bioresour. Technol. 298: 122558. https://doi.org/10.1016/j.biortech.2019.122558.
14. Jędrzejczyk M, Soszka E, Czapnik M, Ruppert AM, Grams J (2019) Physical and chemical pretreatment of lignocellulosic biomass.Second and Third Generation of Feedstocks, pp. 143-196. https://doi.org/10.1016/B978-0-12-815162-4.00006-9.
15. Keshav PK, Shaik N, Koti S, Linga VR (2016) Bioconversion of alkali delignified cotton stalk using two-stage dilute acid hydrolysis and fermentation of detoxified hydrolysate into ethanol. Ind. Crops Prod. 91: 323-331. https://doi.org/10.1016/j.indcrop.2016.07.031.
16. Olivier-Bourbigou H, Magna L, Morvan D (2010) Ionic liquids and catalysis: Recent progress from knowledge to applications. APPL CATAL A-GEN 373: 1-56. https://doi.org/10.1016/j.apcata.2009.10.008.
17. Patel AK, Singhania RR, Sim SJ, Pandey A (2019) Thermostable cellulases: Current status and perspectives. Bioresour. Technol. 279: 385-392. https://doi.org/10.1016/j.biortech.2019.01.049.
18. Rahikainen JL, Martin-Sampedro R, Heikkinen H, Rovio S, Marjamaa K, Tamminen T, Rojas OJ, Kruus K (2013) Inhibitory effect of lignin during cellulose bioconversion: the effect of lignin chemistry on non-productive enzyme adsorption. Bioresour. Technol. 133: 270-278. https://doi-org.libproxy.helsinki.fi/10.1016/j.biortech.2013.01.075.
19. Rocha EGA, Pin TC, Rabelo SC, Costa AC (2017) Evaluation of the use of protic ionic liquids on biomass fractionation. Fuel 206: 145-154. https://doi.org/10.1016/j.fuel.2017.06.014.
20. Roy S, Dikshit PK, Sherpa KC, Singh A, Jacob S, Rajak, RC (2021) Recent nanobiotechnological advancements in lignocellulosic biomass valorization: A review. J. Environ. Manage. 297: 113422. https://doi.org/10.1016/j.jenvman.2021.113422.
21. Samayam IP, Schall CA (2010) Saccharification of ionic liquid pretreated biomass with commercial enzyme mixtures. Bioresour. Technol. 101: 3561-3566. https://doi.org/10.1016/j.biortech.2009.12.066.
22. Turner MB, Spear SK, Huddleston JG, Holbrey JD, Rogers RD (2003) Ionic liquid salt-induced inactivation and unfolding of cellulase from Trichoderma reesei. Green Chem. 5: 443–447. https://doi.org/10.1039/B302570E.
23. Usmani Z, Sharma M, Karpichev Y, Pandey A, Kuhad RC, Bhat R, Punia R, Aghbashlo M, Tabatabaei M, Gupta VK (2020) Advancement in valorization technologies to improve utilization of bio-based waste in bioeconomy context. Renew. Sust. Energ. Rev. 131: 109965. https://doi.org/10.1016/j.rser.2020.109965.

24. Yang J, Ching YC, Chuah CH (2019) Applications of Lignocellulosic Fibers and Lignin in Bioplastics: A Review. Polymers 11: 751. https://doi.org/10.3390/polym11050751.
25. Zhao X, Zhang L, Liu D (2012) Biomass recalcitrance. Part I: the chemical compositions and physical structures affecting the enzymatic hydrolysis of lignocellulose. Biofuel Bioprod. Biorefin. 6: 465-482. https://doi.org/10.1002/bbb.1331.

Figures

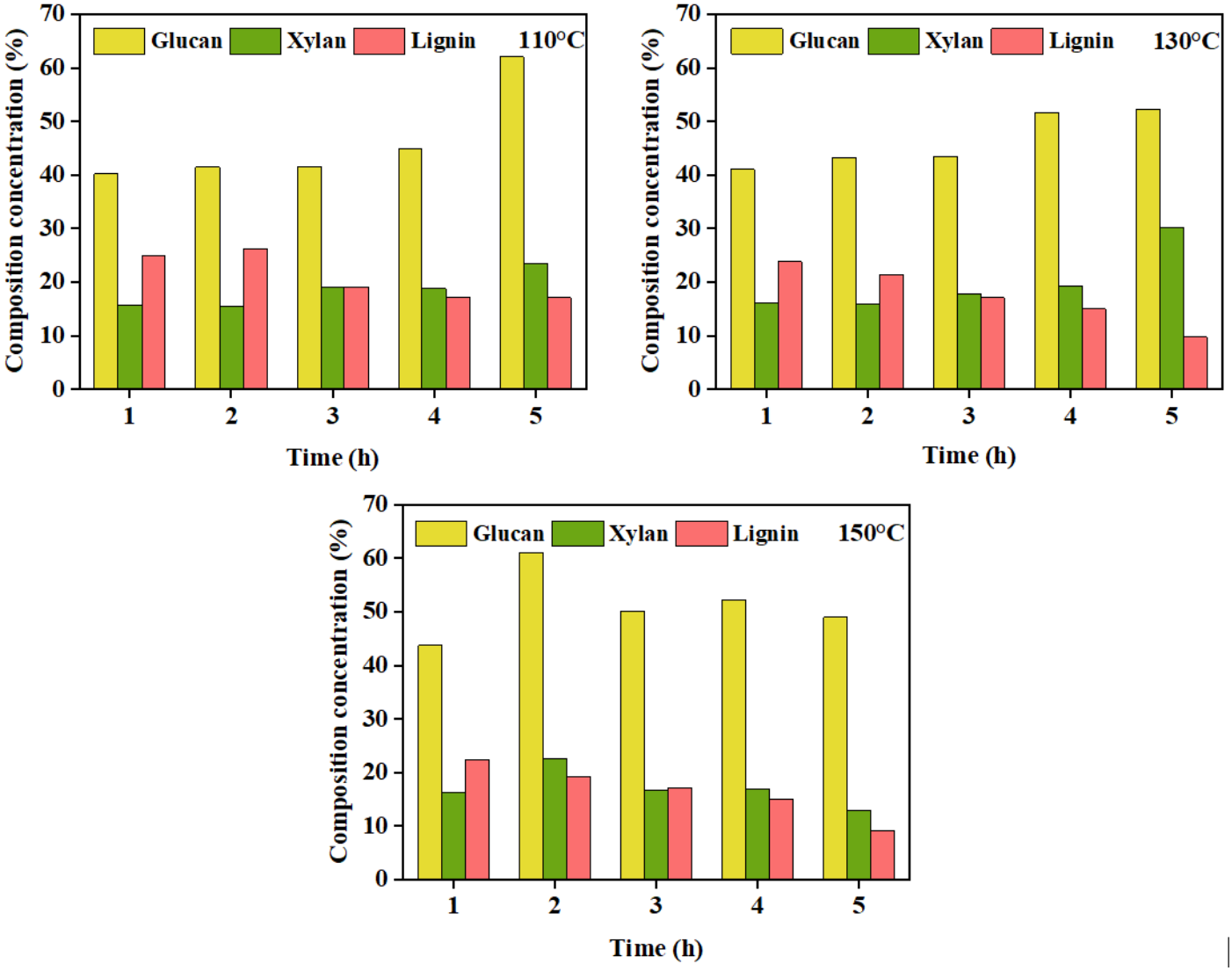

Figure 1

Effect of different pretreatment temperature and time on component content of pretreated CS.

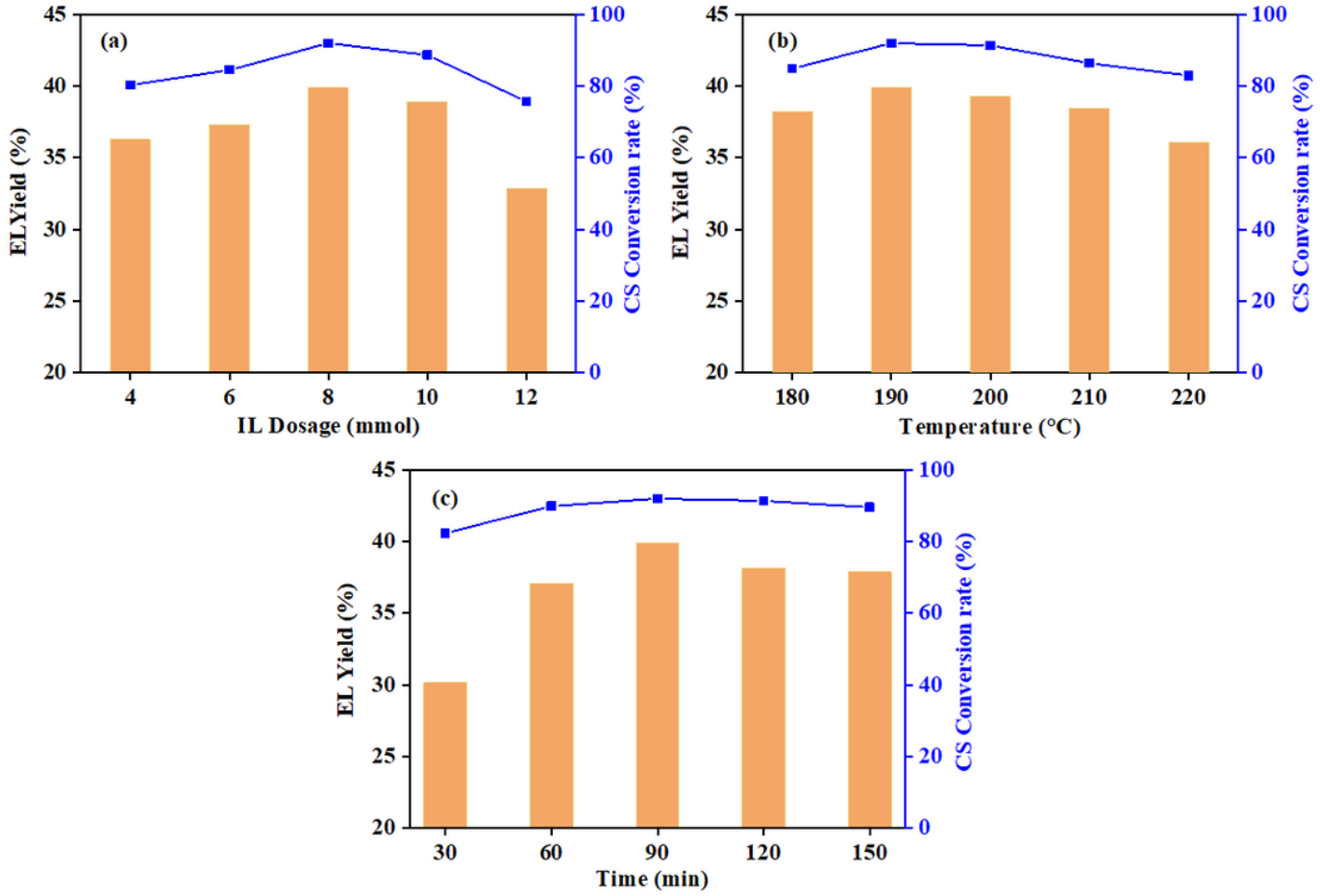

Figure 2

Influence of reaction conditions on the EL yield and CS conversion rate. Reaction conditions: (a) 4 g CS, 190°C, 90 mins; (b) 4 g CS, 8 mmol IL, 90 mins; (c) 4 g CS, 8 mmol IL, 190°C.

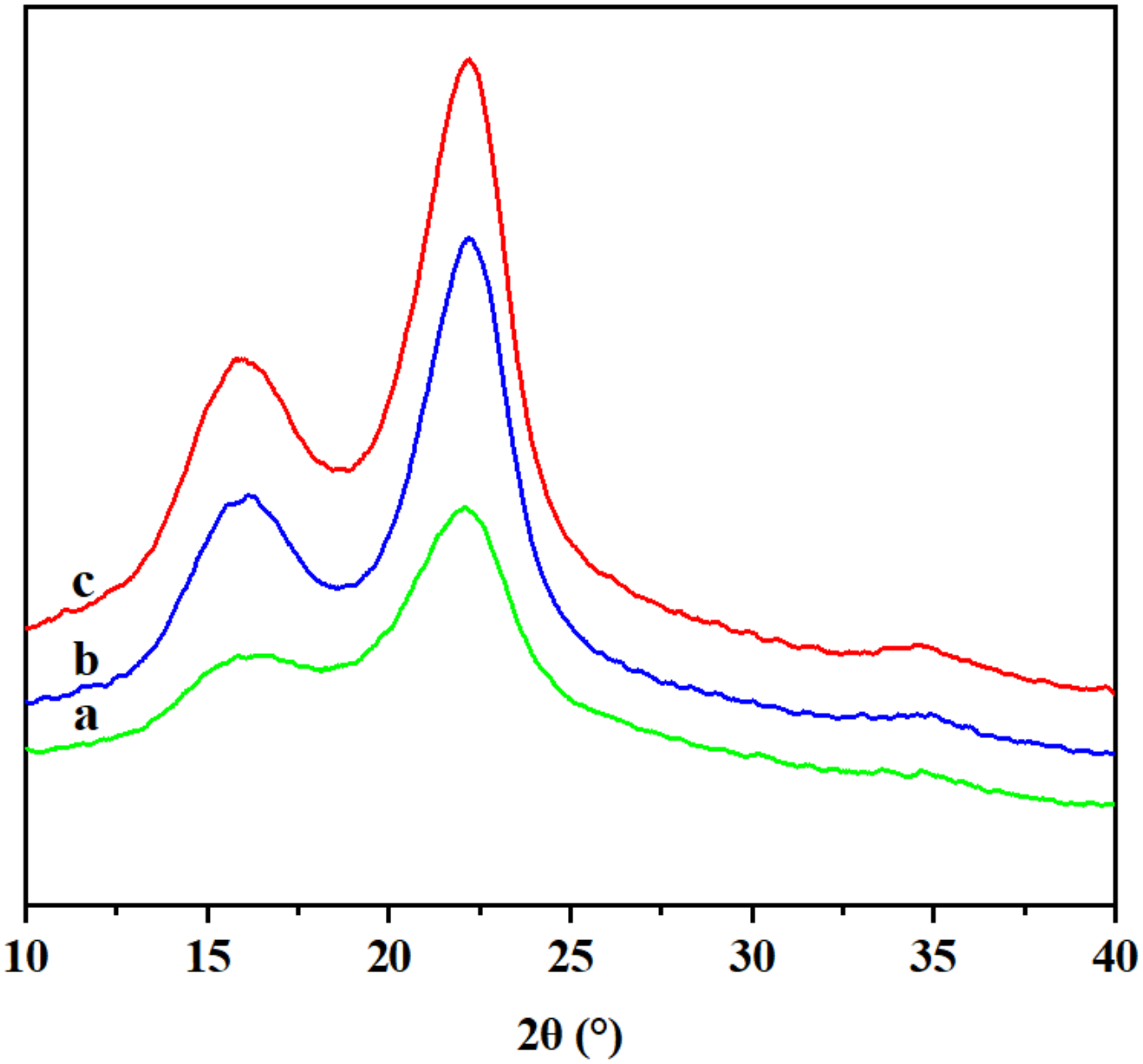

Figure 3

XRD of CS (a), pretreated CS (b) and standard sample (c).

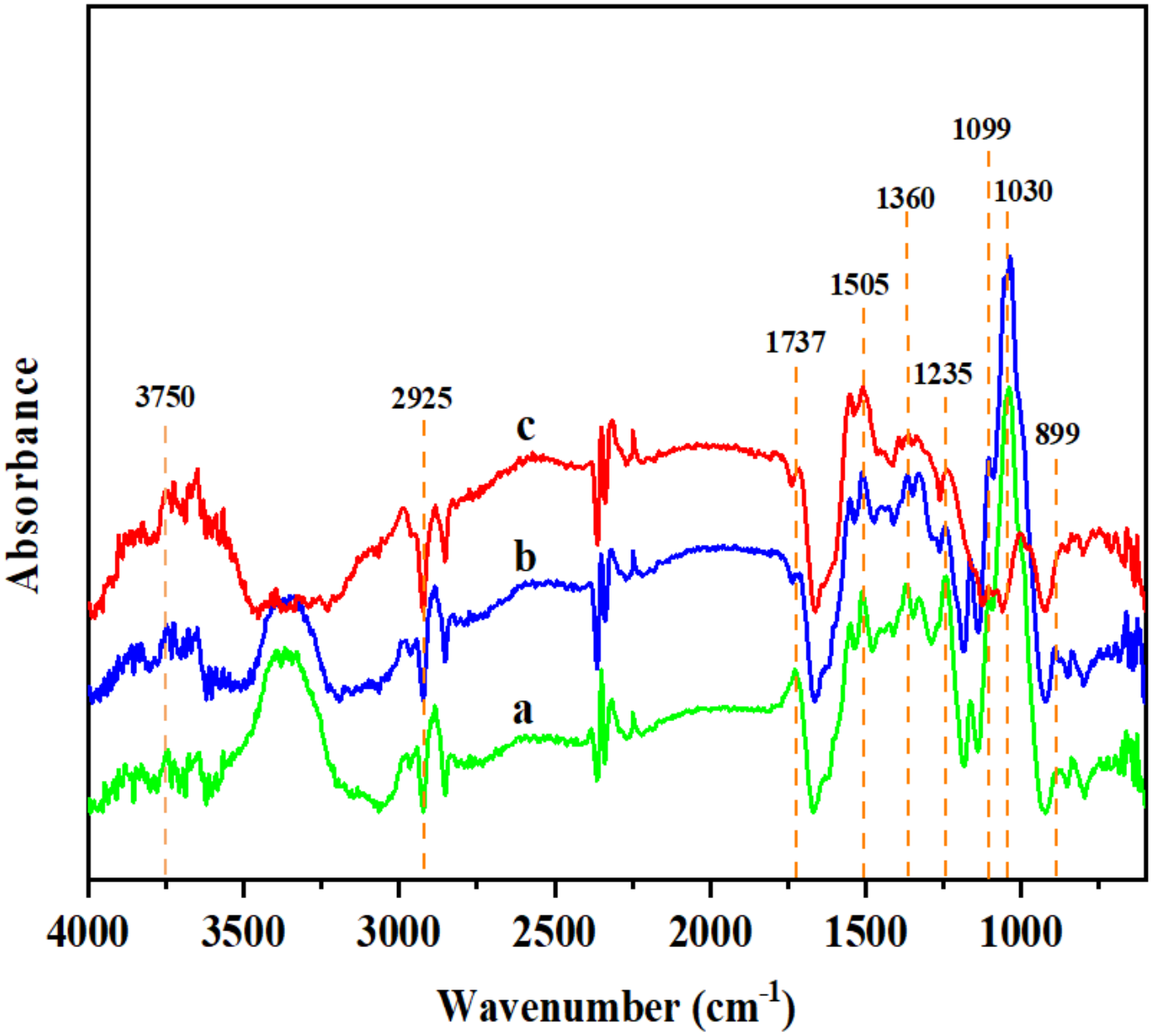

Figure 4

FTIR spectra of CS (a), pretreated CS (b) and RS (c).

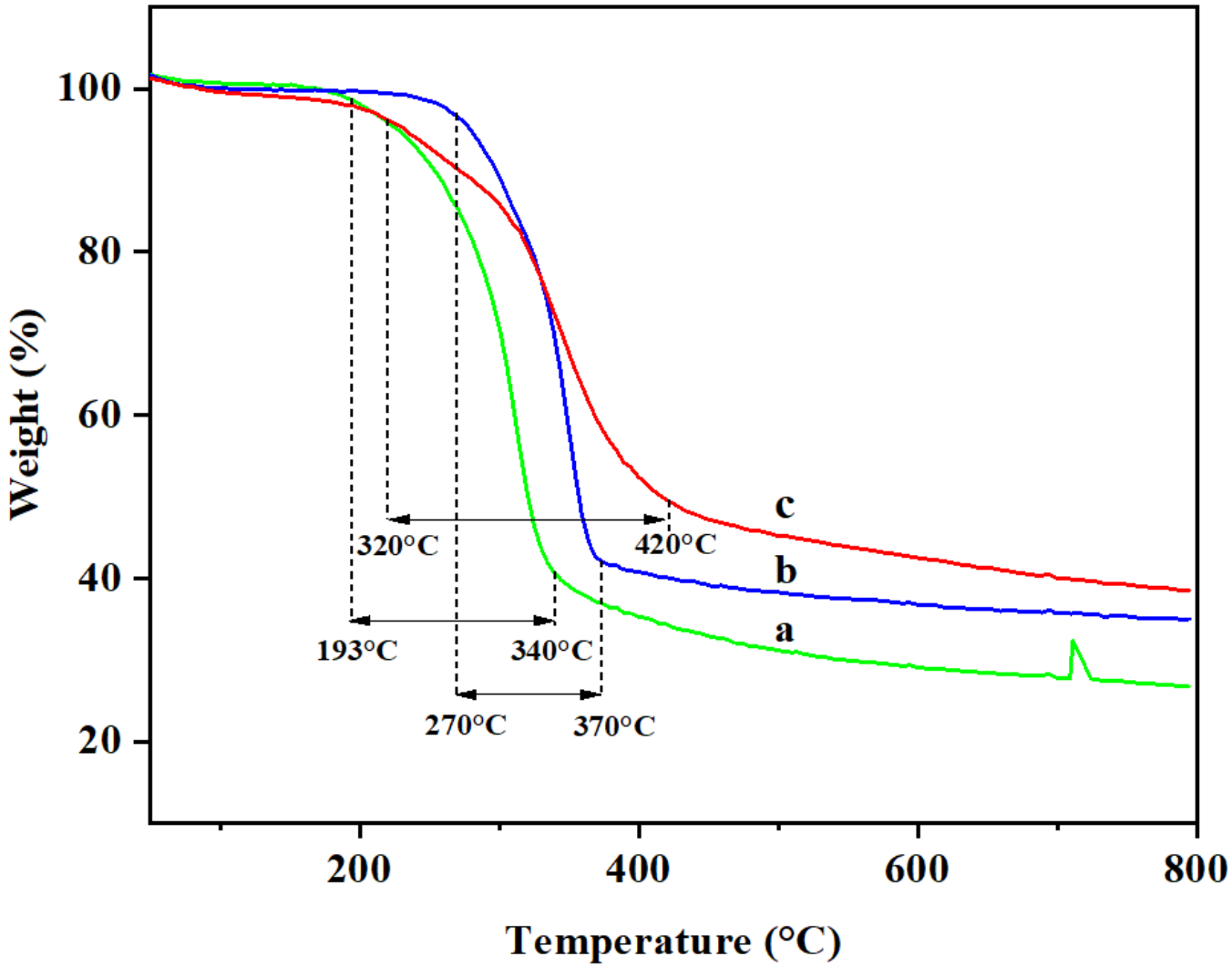

Figure 5

TGA curves of CS (a), pretreated CS (b) and RS (c).

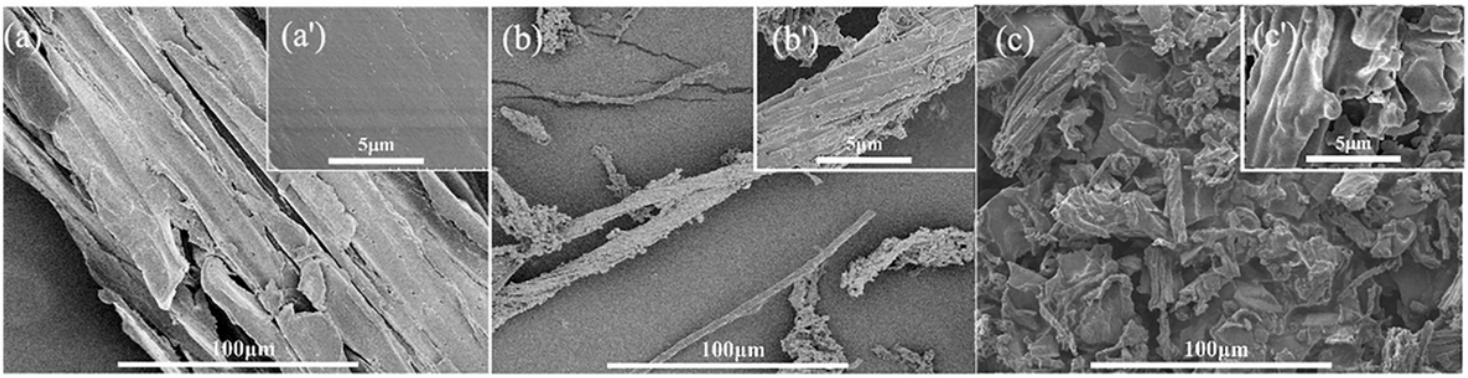

Figure 6

SEM images of CS (a), pretreated CS (b) and RS (c)

Supplementary Files

This is a list of supplementary files associated with this preprint. Click to download.

- GraphicalAbstract.tif